

Real-Time Ground Fault Detection for Inverter-Based Microgrid Systems

Dong, Jingwei; Liao, Yucheng; Xie, Haiwei; Cremer, Jochen; Esfahani, Peyman Mohajerin

DOI

[10.1109/TCST.2024.3458467](https://doi.org/10.1109/TCST.2024.3458467)

Publication date

2025

Document Version

Final published version

Published in

IEEE Transactions on Control Systems Technology

Citation (APA)

Dong, J., Liao, Y., Xie, H., Cremer, J., & Esfahani, P. M. (2025). Real-Time Ground Fault Detection for Inverter-Based Microgrid Systems. *IEEE Transactions on Control Systems Technology*, 33(1), 392-399. <https://doi.org/10.1109/TCST.2024.3458467>

Important note

To cite this publication, please use the final published version (if applicable). Please check the document version above.

Copyright

Other than for strictly personal use, it is not permitted to download, forward or distribute the text or part of it, without the consent of the author(s) and/or copyright holder(s), unless the work is under an open content license such as Creative Commons.

Takedown policy

Please contact us and provide details if you believe this document breaches copyrights. We will remove access to the work immediately and investigate your claim.

Green Open Access added to TU Delft Institutional Repository

'You share, we take care!' - Taverne project

<https://www.openaccess.nl/en/you-share-we-take-care>

Otherwise as indicated in the copyright section: the publisher is the copyright holder of this work and the author uses the Dutch legislation to make this work public.

Real-Time Ground Fault Detection for Inverter-Based Microgrid Systems

Jingwei Dong¹, Yucheng Liao, Haiwei Xie², *Graduate Student Member, IEEE*,
Jochen Cremer¹, *Member, IEEE*, and Peyman Mohajerin Esfahani¹

Abstract—Ground fault detection in inverter-based microgrid (IBM) systems is challenging, particularly in a real-time setting, as the fault current deviates slightly from the nominal value. This difficulty is reinforced when there are partially decoupled disturbances and modeling uncertainties. The conventional solution of installing more relays to obtain additional measurements is costly and also increases the complexity of the system. In this brief, we propose a data-assisted diagnosis scheme based on an optimization-based fault detection filter with the output current as the only measurement. Modeling the microgrid dynamics and the diagnosis filter, we formulate the filter design as a quadratic programming (QP) problem that accounts for decoupling partial disturbances, robustness to nondecoupled disturbances and modeling uncertainties by training with data, and ensuring fault sensitivity simultaneously. To ease the computational effort, we also provide an approximate but analytical solution to this QP. Additionally, we use classical statistical results to provide a thresholding mechanism that enjoys probabilistic false-alarm guarantees. Finally, we implement the IBM system with Simulink and real-time digital simulator (RTDS) to verify the effectiveness of the proposed method through simulations.

Index Terms—Differential-algebraic systems, fault detection, high-fidelity simulator, smart grid.

I. INTRODUCTION

IN THE past decade, inverter-based microgrid (IBM) systems have gained popularity as power systems become increasingly complex and rely more on renewable energy sources [1]. These microgrid systems help integrate renewable energy sources into power systems and regulate the amount of power supplied to customers to provide high-quality power and reduce energy costs. They can also operate independently and allow for local control of distributed generation, for example, when the main grid is unavailable due to blackouts or storms [2]. This greatly increases the reliability of power systems.

Although IBM systems offer many benefits, they are susceptible to faults that can pose safety risks and damage equipment. However, the conventional protection strategy for power systems, such as overcurrent detection, is inefficient in detecting faults in IBM systems [3]. This is because the

fault current only slightly deviates from the nominal value due to a fault current limiter (FCL) embedded in the inverter controller [4]. The fault detection problem is more difficult when considering disturbances that cannot be completely decoupled and modeling uncertainties. Therefore, developing an effective fault detection scheme for IBM systems in the presence of partially decoupled disturbances and modeling uncertainties remains a challenge, particularly when the output current is the only measurement. In this brief, we focus on the detection of ground faults as they are the most common and problematic type of faults in IBM systems [5].

To address the fault detection problem for microgrid systems, researchers have developed several differential methods that rely on communication infrastructure between relays. These methods measure differences in the current symmetrical components [6], the energy content of current [7], the instantaneous current with comparative voltage [8], and the traveling wave polarities [9] to detect faults. Though these methods have shown effectiveness, relying on communication devices can reduce the reliability of systems, and it can be expensive and time-consuming to implement and maintain new equipment. Most recently, to detect ground faults, Pirani et al. [10] provided an optimal input design method ensuring that the output sets of normal and faulty modes of an IBM system are separated with probabilistic guarantees. However, the injected input can degrade system performance, and it is unsuitable for online monitoring due to the intensive computation required for generating the input sequence.

In contrast to differential methods, fault detection methods based on residual generation are less-dependent on the communication infrastructure and additional sensors. Moreover, residual generation-based methods are more suitable for online monitoring than active input design because they do not require continuous updates and have no impact on system performance. In the fault detection field, residual generators are generally constructed using observer-based or parity-space methods [11]. Researchers employ optimization techniques to determine the parameters of residual generators, such that the residuals are sensitive to faults while being robust against disturbances and uncertainties. Alternatively, decomposition techniques such as unknown input observers (UIOs) [12] can be utilized to decouple disturbances from residuals. However, we found that the UIO approach could fail to satisfy the detectability condition when applied to IBM systems with a limited number of measurements.

Nyberg and Frisk [13] proposed a parity-space-like approach to designing residual generators in the framework of linear differential-algebraic equations (DAEs). The derived residual generators can have a lower order than that of the system, thus reducing the computational complexity when dealing

Received 3 April 2024; revised 21 June 2024; accepted 4 September 2024. Date of publication 27 September 2024; date of current version 31 December 2024. This work was supported in part by the European Research Council (ERC) under Grant TRUST-949796 and in part by China Scholarship Council (CSC) under Grant 201806120015. Recommended by Associate Editor V. Puig. (*Corresponding author: Jingwei Dong.*)

Jingwei Dong, Yucheng Liao, and Peyman Mohajerin Esfahani are with Delft Center for Systems and Control, Delft University of Technology, 2628 CD Delft, The Netherlands (e-mail: J.Dong-6@tudelft.nl; Y.Liao-3@student.tudelft.nl; P.MohajerinEsfahani@tudelft.nl).

Haiwei Xie and Jochen Cremer are with the DAI Energy Laboratory, 2628 CD Delft University of Technology, Delft, The Netherlands (e-mail: H.Xie-2@tudelft.nl; J.L.Cremer@tudelft.nl).

Digital Object Identifier 10.1109/TCST.2024.3458467

1063-6536 © 2024 IEEE. Personal use is permitted, but republication/redistribution requires IEEE permission.
See <https://www.ieee.org/publications/rights/index.html> for more information.

with large-scale systems. In addition, this framework provides design freedom in the sense that one can transform the design of residual generators into different optimization problems to obtain desired solutions based on specific requirements. For example, Mohajerin Esfahani and Lygeros [14] reformulated the robust fault detection filter design for nonlinear systems as a quadratic programming (QP) problem to decouple disturbances and minimize the effects of nonlinearity on residuals. Based on this, results for attack detection [15], diagnosis of switched systems [16], and multiple fault estimation [17] have been developed in the DAE framework as well. We would like to emphasize that these methods [14], [15], [16], [17] rely on an accurate system model and all consider disturbances that can be completely decoupled. However, in reality, modeling uncertainties are unavoidable and disturbances generally cannot be completely decoupled, all of which pose challenges to fault diagnosis tasks.

Main Contributions: In this work, we take advantage of the DAE framework to design filters for ground fault detection in the IBM system. To the best of authors' knowledge, this is the first attempt to design fault detection filters within the DAE framework that enables real-time monitoring of ground faults in the IBM system with partially decoupled disturbances and modeling uncertainties. The contributions of this brief are summarized as follows.

- 1) *Dynamic System Modeling:* We develop a unified state-space model for the IBM system in both normal mode and the presence of ground faults (Sections II-B and II-C). This model is further formulated in the DAE framework, which facilitates the design of robust fault detection filters.
- 2) *Data-Assisted Disturbance and Uncertainty Rejection:* To address partially decoupled disturbances and uncertainties, we borrow the idea from [14, Approach (II)] to reframe filter design as a QP problem. The reformulation enables us to decouple partial disturbances, mitigate the effects of nondecoupled disturbances and modeling uncertainties by training with data, and ensure fault sensitivity (Theorem 3.1). Inspiring from [18, Corollary 1], we also obtain an approximate analytical solution to this QP problem with arbitrary accuracy (Corollary 3.3), allowing for online updates of filter parameters.
- 3) *Probabilistic False Alarm Certificate:* Leveraging the classical Markov inequality, we further propose a threshold determination method along with probabilistic false-alarm guarantees (Proposition 3.7).
- 4) *Validation Through a High-Fidelity Simulator:* To validate the effectiveness of the proposed diagnosis scheme, we test it on an IBM system constructed using Simulink and real-time digital simulator (RTDS), which can effectively simulate the practical characteristics of smart grids.

The rest of this brief is organized as follows. The modeling of an IBM system and the problem formulation are presented in Section II. In Section III, we provide the design method for the fault detection filter. In Section IV, we evaluate the effectiveness of the proposed approaches with simulations. Finally, Section V concludes this brief with future directions.

Notation: Sets $\mathbb{R}(\mathbb{R}_+)$ and \mathbb{N} denote all (positive) reals and nonnegative integers, respectively. The space of n -

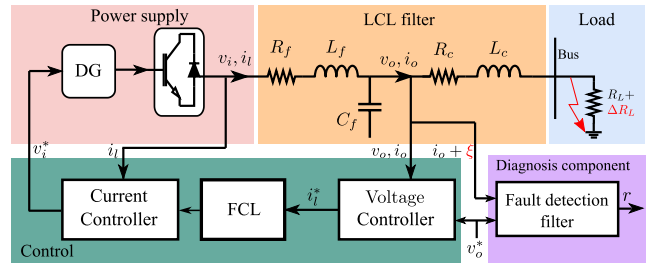


Fig. 1. Architecture of an IBM system with the diagnosis component.

dimensional real-valued vectors is denoted by \mathbb{R}^n . For a vector $v = [v_1, \dots, v_n]$, the infinity norm of v is $\|v\|_\infty = \max_{i \in \{1, \dots, n\}} |v_i|$. The diagonal operator is denoted by $\text{diag}(\cdot)$. For two discrete-time signals s_1 and s_2 taking values in \mathbb{R}^n with length T , the \mathcal{L}_2 inner product is represented as $\langle s_1, s_2 \rangle := \sum_{k=1}^T s_1^\top(k) s_2(k)$, and the corresponding norm $\|s_1\|_{\mathcal{L}_2} := (\langle s_1, s_1 \rangle)^{1/2}$. The notation $\mathbf{0}_{m \times n}$ denotes a zero matrix with m rows and n columns. The identity matrix with an appropriate dimension is denoted by I . For a random variable χ , $\Pr[\chi]$ and $\mathbf{E}[\chi]$ are the probability law and the expectation of χ , respectively.

II. MODELING AND PROBLEM STATEMENT

In this section, we present the state-space model of an IBM system and consider three-phase symmetrical ground faults. Then, we formulate the problem addressed in this work.

A. System Description

An IBM generally consists of four components: the power supplier, the LCL filter, the controller, and the load, as shown in Fig. 1. Let us elaborate on the functions of each component.

- 1) *Power Supplier:* The power supply part contains a generator source and an inverter. We assume that: 1) an ideal generator source is available and 2) the inverter switching process can be neglected due to its high switching frequency. Therefore, we can set the output voltage of the inverter $v_i = v_i^*$. The output current of the inverter is denoted by i_i . As the single generator source supplies all power to the load, droop control is unnecessary, and the microgrid frequency ω is constant.
- 2) *LCL Filter:* The LCL filter is used to filter the harmonics produced by the inverter. It consists of two resistors R_f and R_c , two inductors L_f and L_c , and a capacitor C_f . The signals v_o and i_o denote the grid-side voltage and the output current, respectively.
- 3) *Controller:* The control part keeps the grid-side voltage at v_o^* with two proportional integral (PI) controllers, where v_o^* is a reference voltage determined by load demand and generation capacity. The voltage controller sets reference i_i^* for the current controller. The FCL is a saturation block that protects the microgrid from large fault currents.
- 4) *Load:* The load denoted by R_L is purely resistive, and ΔR_L is the unknown load change.

The mentioned voltages and currents are based on a three-phase system. We introduce the direct-quadrature (dq) transform to simplify the analysis. Specifically, for a three-phase system with current $i = [i_a \ i_b \ i_c]^\top$ and voltage $v = [v_a \ v_b \ v_c]^\top$ in the abc framework, the dq transform projects i

and v onto dq -axis, i.e., $i_{dq} = [i_d \ i_q]^\top = \mathbf{P}i$ and $v_{dq} = [v_d \ v_q]^\top = \mathbf{P}v$. We refer interested readers to [19] for more details about the dq transform.

B. State-Space Model of the Fault-Free IBM System

We first model individual components of the microgrid. Considering the voltage controller in the control component, we transform v_o , v_o^* , i_o , and i_l^* into the dq framework, which are v_{odq} , v_{odq}^* , i_{odq} , and i_{odq}^* , respectively. The cumulative error between v_{odq} and v_{odq}^* denoted by $\phi_{dq} := [\phi_d \ \phi_q]^\top$ can be written as

$$\frac{d\phi_d(t)}{dt} = v_{od}^*(t) - v_{od}(t), \quad \frac{d\phi_q(t)}{dt} = v_{oq}^*(t) - v_{oq}(t). \quad (1)$$

Then, we have the following relations:

$$\begin{cases} \dot{i}_{ld}^* = Fi_{od} - \omega C_f v_{oq} + K_P^v (v_{od}^* - v_{od}) + K_I^v \phi_d \\ \dot{i}_{lq}^* = Fi_{oq} + \omega C_f v_{od} + K_P^v (v_{oq}^* - v_{oq}) + K_I^v \phi_q \end{cases} \quad (2)$$

where F is the feedforward coefficient, and K_P^v and K_I^v denote the proportional and integral gains, respectively. From (1) and (2), we obtain the state-space model of the voltage controller

$$\begin{cases} \dot{\phi}_{dq} = B_{v1} v_{odq}^* + B_{v2} [i_{ldq} \ v_{odq} \ i_{odq}]^\top \\ \dot{i}_{ldq}^* = C_v \phi_{dq} + D_{v1} v_{odq}^* + D_{v2} [i_{ldq} \ v_{odq} \ i_{odq}]^\top \end{cases} \quad (3)$$

where the matrices are

$$\begin{aligned} B_{v1} &= \begin{bmatrix} 1 & 0 \\ 0 & 1 \end{bmatrix}, \quad B_{v2} = \begin{bmatrix} 0 & 0 & -1 & 0 & 0 & 0 \\ 0 & 0 & 0 & -1 & 0 & 0 \end{bmatrix} \\ C_v &= \begin{bmatrix} K_I^v & 0 \\ 0 & K_I^v \end{bmatrix}, \quad D_{v1} = \begin{bmatrix} K_P^v & 0 \\ 0 & K_P^v \end{bmatrix} \\ D_{v2} &= \begin{bmatrix} 0 & 0 & -K_P^v & -\omega C_f & F & 0 \\ 0 & 0 & \omega C_f & -K_P^v & 0 & F \end{bmatrix}. \end{aligned}$$

Similarly, one can obtain the state-space model of the current controller. Let us transform i_l , i_l^* , and v_i^* into the dp framework, which are i_{ldq} , i_{ldq}^* , and v_{idq}^* , respectively. The cumulative error between i_{ldq} and i_{ldq}^* is denoted by $\gamma_{dq} := [\gamma_d \ \gamma_q]^\top$, i.e.,

$$\frac{d\gamma_d(t)}{dt} = i_{ld}^*(t) - i_{ld}(t), \quad \frac{d\gamma_q(t)}{dt} = i_{lq}^*(t) - i_{lq}(t) \quad (4)$$

along with the equations

$$\begin{cases} \dot{v}_{id}^* = -\omega L_f i_{lq} + K_P^c (i_{ld}^* - i_{ld}) + K_I^c \gamma_d \\ \dot{v}_{iq}^* = \omega L_f i_{ld} + K_P^c (i_{lq}^* - i_{lq}) + K_I^c \gamma_q \end{cases} \quad (5)$$

where K_P^c and K_I^c denote the proportional and integral gains, respectively. Based on (4) and (5), the state-space model of the current controller is given by

$$\begin{cases} \dot{\gamma}_{dq} = B_{c1} i_{ldq}^* + B_{c2} [i_{ldq} \ v_{odq} \ i_{odq}]^\top \\ \dot{v}_{idq}^* = C_c \gamma_{dq} + D_{c1} i_{ldq}^* + D_{c2} [i_{ldq} \ v_{odq} \ i_{odq}]^\top \end{cases} \quad (6)$$

where the matrices are

$$\begin{aligned} B_{c1} &= \begin{bmatrix} 1 & 0 \\ 0 & 1 \end{bmatrix}, \quad B_{c2} = \begin{bmatrix} -1 & 0 & \mathbf{0}_{1 \times 4} \\ 0 & -1 & \mathbf{0}_{1 \times 4} \end{bmatrix}, \quad C_c = \begin{bmatrix} K_I^c & 0 \\ 0 & K_I^c \end{bmatrix} \\ D_{c1} &= \begin{bmatrix} K_P^c & 0 \\ 0 & K_P^c \end{bmatrix}, \quad D_{c2} = \begin{bmatrix} -K_P^c & -\omega L_f & \mathbf{0}_{1 \times 4} \\ \omega L_f & -K_P^c & \mathbf{0}_{1 \times 4} \end{bmatrix}. \end{aligned}$$

For the LCL filter, we transform the output voltage of the inverter v_i and the bus voltage v_b into the dq framework,

i.e., v_{idq} and v_{bdq} , respectively. The dynamics of the LCL filter is as follows:

$$\begin{cases} \dot{i}_{ld} = \frac{-R_f}{L_f} i_{ld} + \omega i_{lq} + \frac{1}{L_f} v_{id} - \frac{1}{L_f} v_{od} \\ \dot{i}_{lq} = \frac{-R_f}{L_f} i_{lq} - \omega i_{ld} + \frac{1}{L_f} v_{iq} - \frac{1}{L_f} v_{oq} \\ \dot{v}_{od} = \omega v_{oq} + \frac{1}{C_f} i_{ld} - \frac{1}{C_f} i_{od} \\ \dot{v}_{oq} = -\omega v_{od} + \frac{1}{C_f} i_{lq} - \frac{1}{C_f} i_{oq} \\ \dot{i}_{od} = \frac{-R_c}{L_c} i_{od} + \omega i_{oq} + \frac{1}{L_c} v_{od} - \frac{1}{L_c} v_{bd} \\ \dot{i}_{oq} = \frac{-R_c}{L_c} i_{oq} - \omega i_{od} + \frac{1}{L_c} v_{oq} - \frac{1}{L_c} v_{bq}. \end{cases}$$

Then, the state-space model of the LCL filter becomes

$$\begin{bmatrix} \dot{i}_{ldq} \\ \dot{v}_{odq} \\ \dot{i}_{odq} \end{bmatrix} = A_l \begin{bmatrix} i_{ldq} \\ v_{odq} \\ i_{odq} \end{bmatrix} + [B_{l1} \ B_{l2}] \begin{bmatrix} v_{idq} \\ v_{bdq} \end{bmatrix} \quad (7)$$

where $v_{bdq} = \text{diag}(R_L + \Delta R_L, R_L + \Delta R_L) i_{odq}$, and the matrices are given by

$$\begin{aligned} A_l &= \begin{bmatrix} -\frac{R_f}{L_f} & \omega & -\frac{1}{L_f} & 0 & 0 & 0 \\ -\omega & -\frac{R_f}{L_f} & 0 & -\frac{1}{L_f} & 0 & 0 \\ \frac{1}{C_f} & 0 & 0 & \omega & -\frac{1}{C_f} & 0 \\ 0 & \frac{1}{C_f} & -\omega & 0 & 0 & -\frac{1}{C_f} \\ 0 & 0 & \frac{1}{L_c} & 0 & -\frac{R_c}{L_c} & \omega \\ 0 & 0 & 0 & \frac{1}{L_c} & -\omega & -\frac{R_c}{L_c} \end{bmatrix} \\ B_{l1} &= \begin{bmatrix} \frac{1}{L_f} & 0 & \mathbf{0}_{1 \times 4} \\ 0 & \frac{1}{L_f} & \mathbf{0}_{1 \times 4} \end{bmatrix}^\top \\ B_{l2} &= \begin{bmatrix} \mathbf{0}_{1 \times 4} & -\frac{1}{L_c} & 0 \\ \mathbf{0}_{1 \times 4} & 0 & -\frac{1}{L_c} \end{bmatrix}^\top. \end{aligned}$$

Recalling that $v_{idq} = v_{idq}^*$ and combining (3), (6), and (7), we obtain the complete state-space model of the IBM system in the fault-free case

$$\begin{cases} \dot{x} = A_h x + B_h v_{odq}^* + B_d d \\ i_{odq} = C x \end{cases} \quad (8)$$

where $x = [\phi_{dq}^\top \ \gamma_{dq}^\top \ i_{ldq}^\top \ v_{odq}^\top \ i_{odq}^\top]^\top$ is the augmented state and $d = i_{odq} \Delta R_L$ is the disturbance. The system matrices are

$$A_h = \begin{bmatrix} \mathbf{0}_{2 \times 2} & \mathbf{0}_{2 \times 2} & B_{v2} \\ B_{c1} C_v & \mathbf{0}_{2 \times 2} & B_{c1} D_{v2} + B_{c2} \\ B_{l1} D_{c1} C_v & B_{l1} C_c & A_{h33} \end{bmatrix}$$

$$B_h = \begin{bmatrix} B_{v1} \\ B_{c1}D_{v1} \\ B_{l1}D_{c1}D_{v1} \end{bmatrix}, \quad B_d = \begin{bmatrix} \mathbf{0}_{8 \times 1} & \mathbf{0}_{8 \times 1} \\ -\frac{1}{L_c} & 0 \\ 0 & -\frac{1}{L_c} \end{bmatrix}$$

$$C = [\mathbf{0}_{2 \times 8} \quad I]$$

where

$$A_{h33} = A_l + B_{l1}(D_{c1}D_{v2} + D_{c2}) + B_{l2} \begin{bmatrix} R_L & 0 \\ 0 & R_L \end{bmatrix} [\mathbf{0}_{2 \times 4} \quad I].$$

We would like to highlight that the number of states is 10, while we only have two measurements, i.e., i_{od} and i_{oq} . We take into account disturbances resulting from unknown load changes, which are commonly observed in microgrid systems and typically manifest as random step signals [20], [21], [22]. Therefore, in this study, we assume that d is a step signal taking random values uniformly within the known range $[d_{lb}, d_{ub}]$ where $d_{lb}, d_{ub} \in \mathbb{R}^2$. Additionally, since the dimension of the measurement signal is equal to that of the disturbance, d cannot be fully decoupled [23, Chapter 6], leading to challenges in fault detection. To address this issue, we split $B_d = [\hat{B}_d \check{B}_d]$ and define $d = [\hat{d} \check{d}]^\top$, where \hat{d} and \check{d} represent the decoupled and nondecoupled parts, respectively.

C. State-Space Model of the IBM System With Ground Faults

We consider three-phase symmetrical ground faults, which can cause a short circuit and a sharp increase in currents. After ground faults occur: 1) the bus voltage $v_{bdq} = 0$ because of the short circuit and 2) the output of the voltage controller i_{ldq}^* saturates to a constant value τ_{dq} immediately, i.e., $i_{ldq}^*(t) = \tau_{dq}$ for $t \geq t_f$, where t_f denotes the time instant when ground faults occur. Therefore, the state-space model of the current controller (6) in the faulty mode becomes

$$\begin{cases} \dot{\gamma}_{dq} = B_{c1}\tau_{dq} + B_{c2}[\dot{i}_{ldq} & v_{odq} & i_{odq}]^\top \\ v_{idq}^* = C_c\gamma_{dq} + D_{c1}\tau_{dq} + D_{c2}[\dot{i}_{ldq} & v_{odq} & i_{odq}]^\top. \end{cases} \quad (9)$$

Based on (3), (7), and (9), the state-space model of the IBM system with ground faults can be written as

$$\begin{cases} \dot{x} = A_{uh}x + B_{uh1}v_{odq}^* + B_{uh2}\tau_{dq} \\ i_{odq} = Cx \end{cases} \quad (10)$$

where the matrices A_f , B_{uh1} , and B_{uh2} are

$$A_{uh} = \begin{bmatrix} \mathbf{0}_{2 \times 2} & \mathbf{0}_{2 \times 2} & B_{v2} \\ \mathbf{0}_{2 \times 2} & \mathbf{0}_{2 \times 2} & B_{c2} \\ \mathbf{0}_{6 \times 2} & B_{l1}C_c & A_l + B_{l1}D_{c2} \end{bmatrix}, \quad B_{uh1} = \begin{bmatrix} B_{v1} \\ \mathbf{0}_{2 \times 2} \\ \mathbf{0}_{6 \times 2} \end{bmatrix}$$

$$B_{uh2} = [\mathbf{0}_{2 \times 2} \quad B_{c1}^\top \quad (B_{l1}D_{c1})^\top]^\top.$$

Note that d has no effect on the faulty system because of the short circuit and the redundant state ϕ_{dq} in the faulty model (10) is retained for consistency. To streamline the representation of the normal and faulty models (8) and (10), we introduce a binary signal $f \in \{0, 1\}$, where $f = 1$ indicates the occurrence of ground faults, and $f = 0$ otherwise. Then, we obtain the following unified expression:

$$\begin{cases} \dot{x} = \mathcal{A}(f)x + \mathcal{B}_u(f)u + \mathcal{B}_d(f)d \\ y = Cx \end{cases} \quad (11)$$

where $u = [v_{odq}^* \quad \tau_{dq}^\top]^\top$ and $y = i_{odq}$. The dimensions of x , u , d , and y are denoted by n_x , n_u , n_d , and n_y , respectively. The system matrices are

$$\begin{aligned} \mathcal{A}(f) &= A_h + f(A_{uh} - A_h) \\ \mathcal{B}_u(f) &= [B_h + f(B_{uh1} - B_h) \quad fB_{uh2}] \\ \mathcal{B}_d(f) &= [\hat{B}_d(f) \quad \check{B}_d(f)] = (1-f)[\hat{B}_d \quad \check{B}_d]. \end{aligned}$$

Considering that discrete-time data sampling is used in reality, we discretize the continuous-time state-space model (11) when designing the diagnosis scheme. For convenience, we adopt the same notations for system matrices in both the continuous-time and discrete-time representations.

D. Problem Statement

The objective of this work is to detect the occurrence of ground faults in the IBM system using known signals u and y . Our proposed scheme is to design a residual generator denoted by a linear transfer function \mathbb{F} , whose output is a scalar-valued signal r (called residual). The structure is illustrated in the diagnosis component of Fig. 1. This residual r serves as an indicator of ground faults. Ideally, in the absence of ground faults, r should remain close to zero in the presence of disturbances. However, r can exhibit a significant increase to facilitate detection when ground faults occur.

Additionally, in real-world application scenarios, the measurement \tilde{y} , which is directly fed to the residual generator, may deviate from the output of the mathematical model (MM) y due to simplifications made during the modeling process. Therefore, in addition to disturbances, it is essential to ensure that r remains robust against discrepancies induced by modeling uncertainties, i.e., $\xi = \tilde{y} - y$. Based on the above analysis, to obtain the desired residual behavior, two questions arise naturally. How can we design \mathbb{F} to: 1) mitigate effects of d and ξ on r in the normal mode and 2) enhance fault sensitivity of r in the faulty mode.

In this work, we provide a design method of the filter \mathbb{F} in the DAE framework to fulfill the two requirements. To this end, let us introduce the shift operator q , i.e., $qx(k) = x(k+1)$, and transform the discrete-time version of the unified state-space model (11) into

$$H(q, f)[X] + L(f)[Y] + E(f)[\check{d}] = 0 \quad (12)$$

where $X = [x^\top \hat{d}^\top]^\top$ and $Y = [y^\top u^\top]^\top$. The matrices $H(q, f)$ are a polynomial matrix in q , which is

$$H(q, f) = qH_1 + H_0(f) = \begin{bmatrix} -qI + \mathcal{A}(f) & \hat{B}_d(f) \\ C & \mathbf{0} \end{bmatrix}$$

$$H_1 = \begin{bmatrix} -I & \mathbf{0} \\ \mathbf{0} & \mathbf{0} \end{bmatrix}, \quad H_0(f) = \begin{bmatrix} \mathcal{A}(f) & \hat{B}_d(f) \\ C & \mathbf{0} \end{bmatrix}.$$

The expressions of $L(f)$ and $E(f)$ are

$$L(f) = \begin{bmatrix} \mathbf{0} & B_u(f) \\ -I & \mathbf{0} \end{bmatrix}, \quad E(f) = \begin{bmatrix} \check{B}_d(f) \\ \mathbf{0} \end{bmatrix}.$$

We define $L_0 := L(0)$, $L_1 := L(1)$, and $E_0 := E(0)$ for simplicity of expression.

The fault detection filter \mathbb{F} is defined in the form of

$$F(q) = \frac{N(q)L_0}{a(q)} \quad (13)$$

where the numerator $N(q)$ is a polynomial row vector, i.e., $N(q) = \sum_{i=0}^{d_N} N_i q^i$, $N_i \in \mathbb{R}^{1 \times (n_x + n_y)}$, and d_N is the degree of $N(q)$. The denominator $a(q)$ is a polynomial with a degree larger than d_N and all roots inside the unit circle so that the derived filter is strictly proper and stable. For simplicity of design, we fix d_N and $a(q)$ and only design the coefficients of $N(q)$. It is worth pointing out that $a(q)$ can be chosen up to the user and specific requirements, e.g., noise sensitivity and dynamic performance, which will be our future research.

By setting $f = 0$ and multiplying from the left-hand side of (12) by $a^{-1}(q)N(q)$, we obtain the residual r in the normal mode as

$$\begin{aligned} r &= \frac{N(q)L_0}{a(q)} \begin{bmatrix} \tilde{y} \\ u \end{bmatrix} \\ &= -\frac{N(q)H(q, 0)}{a(q)} [X] - \frac{N(q)E_0}{a(q)} [\check{d}] + \frac{N(q)L_0}{a(q)} [\bar{\xi}] \end{aligned} \quad (14)$$

where $\bar{\xi} = [\bar{\xi}^\top \mathbf{0}^\top]^\top$ as we use the practical measurement \tilde{y} instead of y here.

When ground faults happen, i.e., $f = 1$, DAE model (12) becomes $H(q, 1)[X] + L_1[Y] = 0$ as $E(1) = 0$. It holds that $Y = -L_1^\dagger H(q, 1)[X]$, where L_1^\dagger is the left inverse of L_1 and it always exist as L_1 has full-column rank. The residual r in the faulty mode becomes

$$\begin{aligned} r &= \frac{N(q)L_0}{a(q)} \begin{bmatrix} \tilde{y} \\ u \end{bmatrix} \\ &= -\frac{N(q)L_0 L_1^\dagger H(q, 1)}{a(q)} [X] + \frac{N(q)L_0}{a(q)} [\bar{\xi}]. \end{aligned} \quad (15)$$

Since all the entities in $a^{-1}(q)N(q)L_0[\tilde{y}^\top \ u^\top]^\top$ are known, it can be used to generate the residual. The second line of (14) and (15) characterizes the mapping relations between the unknown signals x, d , and ξ and the residual r in the normal and faulty modes, respectively, based on which we can design $N(q)$ for different diagnosis purposes.

Recall the two design requirements. To ensure a sufficiently small residual, we decouple X from r when there is no fault through

$$N(q)H(q, 0)|_{q=1} = 0. \quad (16a)$$

Furthermore, we let the transfer function from X to r remain nonzero to guarantee fault sensitivity in the faulty mode, i.e.,

$$N(q)L_0 L_1^\dagger H(q, 1)|_{q=1} \neq 0. \quad (16b)$$

We also aim to mitigate the effects of ξ on r , namely, the last term in (14) and (15). Inspired by the approach in [14], we tackle this problem from a data-driven perspective by training the filter with historical data of ξ to enhance its robustness. To elaborate, we can obtain $m \in \mathbb{N}$ instances of output differences, i.e., $\{\xi_1, \dots, \xi_m\}$, by running the actual system and the MM simultaneously. For each instance $\xi_i = [\xi_i(0), \xi_i(1), \dots, \xi_i(T)]$ with $T \in \mathbb{N}$, we define

its contribution to r as

$$r_{\xi_i} = \frac{N(q)L_0}{a(q)} [\bar{\xi}_i], \quad \bar{\xi}_i = [\xi_i^\top \ \mathbf{0}^\top]^\top.$$

Then, we can suppress the average effects of ξ by constraining the \mathcal{L}_2 -norm of r_{ξ_i} for all $i \in \{1, \dots, m\}$, i.e.,

$$\frac{1}{m} \sum_{i=1}^m \|r_{\xi_i}\|_{\mathcal{L}_2}^2 = \frac{1}{m} \sum_{i=1}^m \left\| \frac{N(q)L_0}{a(q)} [\bar{\xi}_i] \right\|_{\mathcal{L}_2}^2 \leq \beta_1 \quad (16c)$$

where $\beta_1 \in \mathbb{R}_+$. We show later the approach to constructing $\|r_{\xi_i}\|_{\mathcal{L}_2}^2$ with a combination of the system model and historical data. For the nondecoupled disturbance \check{d} in (14), we choose the same solution as above and let

$$\frac{1}{m} \sum_{i=1}^m \|r_{\check{d}_i}\|_{\mathcal{L}_2}^2 = \frac{1}{m} \sum_{i=1}^m \left\| \frac{N(q)E_0}{a(q)} [\check{d}_i] \right\|_{\mathcal{L}_2}^2 \leq \beta_2 \quad (16d)$$

where $\beta_2 \in \mathbb{R}_+$, \check{d}_i for $i \in \{1, \dots, m\}$ is an instance of \check{d} , and $r_{\check{d}_i}$ denotes the contribution of \check{d}_i to r .

Problem (Data-Assisted Robust Fault Detection Filter Design): Consider the state-space model of the IBM system (11) with three-phase symmetrical ground faults. Given m instances of output discrepancies ξ_i and nondecoupled disturbances \check{d}_i , find a fault detection filter \mathbb{F} in the form of (13) that satisfies (16a)–(16d).

III. MAIN RESULTS

In this section, we present the design method of the fault detection filter and the determination method of the threshold.

A. Filter Design

Let us start by constructing $\|r_{\xi_i}\|_{\mathcal{L}_2}^2$ mentioned above. Note that the response of the j th element of ξ_i , i.e., $\xi_i(j)$, can be computed by

$$[r_{\xi_i(j)}(0), r_{\xi_i(j)}(1), \dots, r_{\xi_i(j)}(T)] = N(q)L_0 \bar{\xi}_i(j) \bar{\ell}_j$$

where $\bar{\ell}_j = \overbrace{[0, \dots, 0, \ell(0), \ell(1), \dots, \ell(T-j)]}^j$ and $\ell(k)$ for $k \in \mathbb{N}$ is the value of the discrete-time unit impulse response of $a^{-1}(q)$ at the time instance k . By summing up the response of $\xi_i(j)$ for $j \in \{0, \dots, T - d_N\}$, we obtain

$$\begin{aligned} [r_{\xi_i}(0), r_{\xi_i}(1), \dots, r_{\xi_i}(T)] \\ &= N(q)L_0 \sum_{j=0}^{T-d_N} \bar{\xi}_i(j) \bar{\ell}_j \\ &= \bar{N} \bar{L}_0 \begin{bmatrix} I \\ qI \\ \vdots \\ q^{d_N} I \end{bmatrix} [\bar{\xi}_i(0), \dots, \bar{\xi}_i(T - d_N)] \begin{bmatrix} \bar{\ell}_0 \\ \vdots \\ \bar{\ell}_{T-d_N} \end{bmatrix} \end{aligned} \quad (17)$$

where $\bar{N} = [N_0, N_1, \dots, N_{d_N}]$ and $\bar{L}_0 = \text{diag}(L_0, \dots, L_0)$ according to the multiplication rule of polynomial matrices [14, Lemma 4.2]. Recall that q is a time-shift operator,

i.e., $q\bar{\xi}_i(k) = \bar{\xi}_i(k+1)$. Equation (17) becomes

$$\begin{aligned} & [r_{\xi_i}(0), r_{\xi_i}(1), \dots, r_{\xi_i}(T)] \\ &= \bar{N}\bar{L}_0 \begin{bmatrix} \bar{\xi}_i(0) & \dots & \bar{\xi}_i(T-d_N) \\ \bar{\xi}_i(1) & \dots & \bar{\xi}_i(T-d_N+1) \\ \vdots & \ddots & \vdots \\ \bar{\xi}_i(d_N) & \dots & \bar{\xi}_i(T) \end{bmatrix} \begin{bmatrix} \bar{\ell}_0 \\ \vdots \\ \bar{\ell}_{T-d_N} \end{bmatrix} \\ &= \bar{N}\bar{L}_0\Xi_i\Gamma. \end{aligned} \quad (18)$$

To ensure the existence of Ξ_i , we assume that the length of data T is greatly larger than d_N+1 , i.e., $T \gg d_N+1$. With (18), $\|r_{\xi_i}\|_{\mathcal{L}_2}^2$ is further formulated into

$$\|r_{\xi_i}\|_{\mathcal{L}_2}^2 = \bar{N}\Phi_i\bar{N}^\top, \quad \Phi_i = \bar{L}_0\Xi_i\Gamma(\bar{L}_0\Xi_i\Gamma)^\top. \quad (19)$$

It is worth emphasizing that Φ_i is positive semidefinite since $\|r_{\xi_i}\|_{\mathcal{L}_2}^2 = \bar{N}\Phi_i\bar{N}^\top \geq 0$ for all nonzero \bar{N} . Similarly, we obtain the signature matrix for \check{d}_i , which is

$$\|r_{\check{d}_i}\|_{\mathcal{L}_2}^2 = \bar{N}\Psi_i\bar{N}^\top, \quad \Psi_i = \bar{E}_0\check{D}_i\Gamma(\bar{E}_0\check{D}_i\Gamma)^\top.$$

The construction of \bar{E}_0 and \check{D}_i is similar to that of \bar{L}_0 and Ξ_i .

Now, we can present the design method of the ground fault detection filter for the IBM system in the following theorem.

Theorem 3.1 (Filter design: QP): Consider the unified state-space model of the IBM system (11) and the structure of the fault detection filter in (13). Given the degree d_N , a stable $a(q)$, and m instances of output discrepancies ξ_i and nondecoupled disturbances \check{d}_i , (16a)–(16d) in problem are satisfied by solving the following optimization problem:

$$\begin{aligned} & \min_{\bar{N}} \bar{N}(\bar{\Phi} + \bar{\Psi})\bar{N}^\top - \|\bar{N}\bar{L}\bar{H}(1)\bar{I}\|_\infty \\ & \text{s.t. } \bar{N}\bar{H}(0)\bar{I} = 0 \end{aligned} \quad (20)$$

where $\bar{\Phi} = (1/m) \sum_{i=1}^m \Phi_i$, $\bar{\Psi} = (1/m) \sum_{i=1}^m \Psi_i$,

$$\begin{aligned} \bar{L} &= \text{diag}(\underbrace{L_0L_1^\dagger, \dots, L_0L_1^\dagger}_{d_N+1}, \underbrace{I, \dots, I}_{d_N+2})^\top \\ \bar{H}(f) &= \begin{bmatrix} H_0(f) & H_1 & 0 & \dots & 0 \\ 0 & H_0(f) & H_1 & 0 & \vdots \\ \vdots & 0 & \ddots & \ddots & 0 \\ 0 & \dots & 0 & H_0(f) & H_1 \end{bmatrix}, \quad f \in \{0, 1\}. \end{aligned}$$

Proof: According to the multiplication rule of polynomial matrices, we have

$$\begin{aligned} N(q)H(q, 0) &= \bar{N}\bar{H}(0)[I, qI, \dots, q^{d_N+1}I]^\top \\ N(q)L_0L_1^\dagger H(q, 1) &= \bar{N}\bar{L}\bar{H}(1)[I, qI, \dots, q^{d_N+1}I]^\top. \end{aligned}$$

One can see from the first equality that, by letting $q = 1$, $\bar{N}\bar{H}(0)\bar{I} = 0$ directly implies (16a). For (16b), we let coefficients of $N(q)L_0L_1^\dagger H(q, 1)$ be nonzero by maximizing $\|\bar{N}\bar{L}\bar{H}(1)\bar{I}\|_\infty$ in the objective function, such that (16b) is satisfied. The first term in the objective function, i.e., $\bar{N}(\bar{\Phi} + \bar{\Psi})\bar{N}^\top$, relates to (16c) and (16d), which ensures that the average effects of different instances of ξ and \check{d} on r are bounded. The derivation process of the quadratic form of $\|r_{\xi_i}\|_{\mathcal{L}_2}^2$ and $\|r_{\check{d}_i}\|_{\mathcal{L}_2}^2$ is presented in (17)–(19). This completes the proof. \square

Note that $\bar{N}\bar{L}\bar{H}(1)\bar{I}$ is a row vector with $(n_x + 1)$ columns. For a positive scalar ζ , $\|\bar{N}\bar{L}\bar{H}(1)\bar{I}\|_\infty \geq \zeta$ holds if and only if $\bar{N}\bar{L}\bar{H}(1)\bar{I}e_i \geq \zeta$ or $\bar{N}\bar{L}\bar{H}(1)\bar{I}e_i \leq -\zeta$, where e_i

is an $(n_x + 1)$ -dimensional column vector with only the i th element be 1 and the rest are zero, i.e., $e_i = [0, \dots, 1, \dots, 0]^\top$. Moreover, it is easy to check that if \bar{N}^* is a solution to (20), so is $-\bar{N}^*$. Additionally, Φ_i and Ψ_i are positive semidefinite. Therefore, (20) can be viewed as a set of $(n_x + 1)$ QP problems by replacing the term $\|\bar{N}\bar{L}\bar{H}(1)\bar{I}\|_\infty$ with $\bar{N}\bar{L}\bar{H}(1)\bar{I}e_i$ (or $-\bar{N}\bar{L}\bar{H}(1)\bar{I}e_i$), and thus is convex and tractable.

Remark 3.2 (Feasibility Analysis): It holds that $(d_N + 1)(n_x + n_y) = \text{Rank}(\bar{H}(0)\bar{I}) + \text{Null}(\bar{H}(0)\bar{I})$ based on Rank Plus Nullity theorem, where $\text{Rank}(\bar{H}(0)\bar{I})$ and $\text{Null}(\bar{H}(0)\bar{I})$ denote the rank and the left null space dimension of $\bar{H}(0)\bar{I}$, respectively. Thus, the equality constraint in (20) is feasible when $(d_N + 1)(n_x + n_y) > \text{Rank}(\bar{H}(0)\bar{I})$, i.e., $\text{Null}(\bar{H}(0)\bar{I}) \neq 0$. For $\|\bar{N}\bar{L}\bar{H}(1)\bar{I}\|_\infty \neq 0$, it requires that $\bar{L}\bar{H}(1)\bar{I}$ does not belong to the column range space of $\bar{H}(0)\bar{I}$, i.e., $\text{Rank}(\bar{H}(0)\bar{I} \bar{L}\bar{H}(1)\bar{I}) > \text{Rank}(\bar{H}(0)\bar{I})$. Otherwise, a feasible \bar{N} to $\bar{N}\bar{H}(0)\bar{I} = 0$ leads to $\bar{N}\bar{L}\bar{H}(1)\bar{I} = 0$.

We further propose an approximate analytical solution to (20) in the following corollary.

Corollary 3.3 (Approximate Analytical Solution):

Consider the optimization problem (20). There exists an approximate analytical solution given in the following form:

$$\bar{N}^*(\delta) = \frac{(\bar{L}\bar{H}(1)\bar{I}e_i^*)^\top}{2\delta} (\delta^{-1}(\bar{\Phi} + \bar{\Psi}) + \bar{H}(0)\bar{I}\bar{I}^\top\bar{H}^\top(0))^{-1} \quad (21)$$

where $e_i^* = \arg \max_{i \in \{1, \dots, n_x+1\}} |\bar{N}^*(\delta)\bar{L}\bar{H}(1)\bar{I}e_i|$ and $\delta \in \mathbb{R}_+$ is the Lagrange multiplier. The solution $\bar{N}^*(\delta)$ provides an approximate solution to (20) and will converge to the optimal solution as δ tends to ∞ .

Proof: The proof is similar to that of [18, Corollary 3.4] and thus is omitted here. \square

With the analytical solution, one can update the coefficients of the filter online with new data without the need to resolve (20), which is an improvement over [14].

Remark 3.4 (Average Objective Function): We consider the average effects of all ξ_i and \check{d}_i on the residual as the objective function in (20). An alternative way is to consider the worst-case scenario, i.e., $\max_{i \in \{1, \dots, m\}} \bar{N}(\Phi_i + \Psi_i)\bar{N}^\top$. The average objective function is, however, of interest if one requires to train the filter with a large number of patterns. This is due to the fact that the computational complexity of the derived QP problem is independent of the number of instances with the average objective function.

Remark 3.5 (Approximate Analytical Solution With δ):

The Lagrange multiplier δ is introduced in (20) to penalize the equality constraint $\bar{N}\bar{H}(0)\bar{I} = 0$, and in the ideal case, δ tends to infinity as stated in Corollary 3.3. However, for a bounded δ , the equality constraint cannot be strictly satisfied, which is why we refer to the solution (21) as an approximate analytical solution. Additionally, to ensure that $\bar{N}\bar{H}(0)\bar{I}$ is sufficiently close to zero, δ should be large enough while remaining numerically bounded for practical considerations.

Remark 3.6 (Control Saturation): In our problem, we adopt PI controllers in the IBM system, which may raise concerns about control saturation. We would like to highlight that since we consider a small-signal model of the IBM system with bounded load changes, controller saturation is rare and not a major problem we aimed to deal with. Nonetheless, in the case of saturation, we can address this

issue by modeling the IBM system with saturation and incorporating the disturbance suppression when saturation happens in design conditions.

To detect the fault, we introduce the power of the residual $r(k)$ as the evaluation function, i.e., $J(r) = r(k)^2$ for $k \in \mathbb{N}$. Let J_{th} be the detection threshold. Then, we can consider the following detection logic:

$$\begin{cases} J(r) \leq J_{th} & \Rightarrow \text{no faults} \\ J(r) > J_{th} & \Rightarrow \text{faults.} \end{cases}$$

We show the computation method of the threshold and the false alarm rate in the following proposition.

Proposition 3.7 (Probabilistic False Alarm Certificate):

Assume that the patterns of \check{d} and ξ follow different independent identically distributed (i.i.d.) distributions. Consider (11), the filter $\mathbb{F}(q)$ obtained by solving (20) with the corresponding optimal solution \bar{N}^* , and the evaluation function $J(r) = r(k)^2$. Given a scalar $\lambda \geq 1$, if we set the threshold J_{th} as

$$J_{th} = \frac{\lambda}{T} \bar{N}^* (\bar{\Phi} + \bar{\Psi}) \bar{N}^{*\top} \quad (22)$$

the false alarm rate in the steady state satisfies

$$\lim_{k \rightarrow \infty} \Pr\{J(r(k)) > J_{th} | f = 0\} \leq \frac{1}{\lambda}. \quad (23)$$

Proof: Since both \check{d}_i and ξ_i follow i.i.d. distributions, the residual in the normal mode as shown in (14) can be viewed as a random variable. It is proven in [14, Theorem 4.11] that the empirical average error

$$\varepsilon_m = \frac{1}{m} \sum_{i=1}^m \|r_{\xi_i} + r_{\check{d}_i}\|_{\mathcal{L}_2}^2 - \mathbf{E}[\|r\|_{\mathcal{L}_2}^2]$$

satisfies the strong law of large numbers, i.e., $\lim_{m \rightarrow \infty} \varepsilon_m = 0$ almost surely. Therefore, in the steady state, it holds that

$$\begin{aligned} J_{th} &= \lim_{T, m \rightarrow \infty} \frac{\lambda}{T} \left(\frac{1}{m} \sum_{i=1}^m \|r_{\xi_i}\|_{\mathcal{L}_2}^2 + \frac{1}{m} \sum_{i=1}^m \|r_{\check{d}_i}\|_{\mathcal{L}_2}^2 \right) \\ &\geq \lim_{T, m \rightarrow \infty} \frac{\lambda}{T} \left(\frac{1}{m} \sum_{i=1}^m \|r_{\xi_i} + r_{\check{d}_i}\|_{\mathcal{L}_2}^2 \right) \\ &= \lim_{T \rightarrow \infty} \frac{\lambda}{T} \mathbf{E}[\|r\|_{\mathcal{L}_2}^2] = \lambda \lim_{k \rightarrow \infty} \mathbf{E}[r(k)^2]. \end{aligned}$$

According to Markov inequality, the false alarm rate in the steady state satisfies

$$\begin{aligned} &\lim_{k \rightarrow \infty} \Pr\{r(k)^2 > J_{th} | f = 0\} \\ &< \lim_{k \rightarrow \infty} \Pr\{r(k)^2 > \lambda \mathbf{E}[r(k)^2] | f = 0\} \leq \frac{1}{\lambda}. \end{aligned}$$

This completes the proof. \square

We further derive the circumstances in which ground faults can be detected by comparing the steady-state value of r^2 with J_{th} . However, given that the faulty model is unobservable, it is essential to first identify its observable subsystem, denoted as $(A_{uh,o}, [B_{uh1,o}, B_{uh2,o}], C_{uh,o})$, through Kalman decomposition. Define the transfer function from $[v_{odq}^* \ \tau_{dq}]^\top$ to r as $\mathcal{T}_{ur}(q) = C_{uh,o}(qI - A_{uh,o})^{-1}[B_{uh1,o}, B_{uh2,o}]$. Then, the ground faults can be detected if

$$\left(\frac{N(q)L_0}{a(q)} \begin{bmatrix} \mathcal{T}_{ur}(q) \\ I \end{bmatrix} \begin{bmatrix} v_{odq}^* \\ \tau_{dq} \end{bmatrix} \Big|_{q=1} \right)^2 > J_{th}.$$

TABLE I
PARAMETERS

Initial Conditions				Microgrid Parameters			
v_{od}	380.8	i_{ld}	11.4	ω	314.1	R_L	12 Ω
v_{oq}	0	i_{lq}	-5.5×10^3	L_f	3.5 mH	K_P^c	0.3
i_{od}	11.4	v_{bd}	379.5	R_f	0.01 Ω	K_I^c	20
i_{oq}	0.4	v_{bq}	-6	C_f	21.9 μ F	K_P^v	2
ϕ_d	0.13	γ_d	0.0115	L_c	1.3 mH	K_I^v	14
ϕ_q	0	γ_q	0	R_c	0.02 Ω	F	0.75

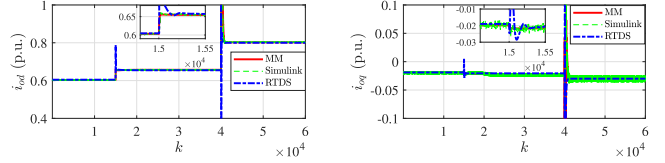


Fig. 2. Output currents generated by different models.

IV. NUMERICAL RESULTS IN RTDS

In this section, we validate the performance of the fault detection filter through simulations. We refer interested readers to the extended version of this work [24] for additional simulation results. Here, we report only the results implemented with the IBM system depicted in Fig. 1 through the MM (11), Simulink, and RTDS. Note that electrical components integrated into Simulink and RTDS allow for a more realistic simulation of practical scenarios compared to the simplified MM. In addition, RTDS is widely recognized in the industry for its ability to simulate power systems in real time [25]. Subsequently, we collect the discrepancy data between the output of MM and those from Simulink and RTDS. Step signals are employed to characterize the unknown load changes. Following this, we design the filter by solving the optimization problem (20). Finally, we apply the derived filter to models constructed by Simulink and RTDS to evaluate diagnosis performance in the presence of partially decoupled disturbances and modeling uncertainties.

The parameters of the system are presented in Table I, sourced from [26] with some modifications. The sampling period is 0.1 ms and the simulation time is 6 s. The reference frequency and reference voltage are 50 Hz and $v_{odq}^* = [3810]^\top$, respectively. The FCL parameter is $\tau_{dq} = [35, 0.7]^\top$. To design the fault detection filter following the structure of (13), we set the degree of $N(q)$ as $d_N = 10$ and choose a stable denominator $a(q)$ with a degree larger than d_N . We further collect 100 output discrepancy and disturbance instances with $T = 200$ to construct $\bar{\Phi}$ and $\bar{\Psi}$, respectively. The disturbance is a step signal, i.e., $d = [-15 \ 0.1]^\top$ for $k > 15000$. The ground fault occurs at $k = 40000$. Given the settings specified above, we utilize the YALMIP toolbox [27] to address the optimization problem (20) and obtain the fault detection filter. The simulation results are presented in Figs. 2 and 3.

Fig. 2 illustrates the per-unit (p.u.) values of output currents generated by the three different models, which exhibit close resemblance. This implies that the simplified MM aligns well with the more intricate systems constructed using Simulink and RTDS. From the small figures, one can see minor discrepancies between these outputs. Furthermore, there is a step change in the output currents after an unknown load change

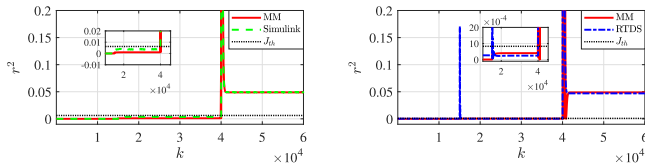


Fig. 3. Diagnosis results with different models.

at $k = 15000$, which is similar to the effect caused by the ground fault at $k = 40000$. Therefore, discerning the occurrence of a ground fault solely from the output current proves challenging.

Fig. 3 displays the diagnosis results characterized through the values of $r^2(k)$. In the left figure, we show the diagnostic performance of the filter designed to withstand output discrepancies between MM and the Simulink model. One can see that $r^2(k)$ remains below the threshold in the presence of partially decoupled disturbances and modeling uncertainties until the occurrence of the fault at $k = 40000$. After the fault occurs, $r^2(k)$ immediately exceeds the threshold and remains higher than the threshold. This indicates that the fault is successfully detected with modeling uncertainties and is distinguishable from disturbances. The right-hand side figure depicts the diagnosis outcome of the filter designed for the RTDS model. One can see that this filter effectively suppresses the partially decoupled disturbances and modeling uncertainties and successfully detects the ground fault as well. Note that due to the spike induced by the load change in the output current, $r^2(k)$ surpasses the threshold and causes a false alarm. Nonetheless, the signal rapidly diminishes below the threshold, distinguishing it from scenarios where ground faults occur. To address this issue, we can extend the evaluation time.

V. CONCLUSION

In this brief, we propose a diagnosis scheme for the detection of ground faults in IBM systems with partially decoupled disturbances and modeling uncertainties. In future work, we first will consider designing the denominator of the filter for better dynamic performance. The second direction will be focused on extending the proposed approaches to more complex and realistic settings, such as considering the presence of multiple converters.

ACKNOWLEDGMENT

The authors are grateful to M. Popov and A. Lekic for the valuable discussion on IBM systems.

REFERENCES

- [1] M. W. Altaf, M. T. Arif, S. N. Islam, and M. E. Haque, "Microgrid protection challenges and mitigation approaches—A comprehensive review," *IEEE Access*, vol. 10, pp. 38895–38922, 2022.
- [2] M. A. Zamani, A. Yazdani, and T. S. Sidhu, "A communication-assisted protection strategy for inverter-based medium-voltage microgrids," *IEEE Trans. Smart Grid*, vol. 3, no. 4, pp. 2088–2099, Dec. 2012.
- [3] K. Lai, M. S. Illindala, and M. A. Haj-ahmed, "Comprehensive protection strategy for an islanded microgrid using intelligent relays," in *Proc. IEEE Ind. Appl. Soc. Annu. Meeting*, Oct. 2015, pp. 1–11.
- [4] H. Karimi, G. Shahgholian, B. Fani, I. Sadeghkhani, and M. Moazzami, "A protection strategy for inverter-interfaced islanded microgrids with looped configuration," *Electr. Eng.*, vol. 101, no. 3, pp. 1059–1073, Sep. 2019.
- [5] T. Loix, T. Wijnhoven, and G. Deconinck, "Protection of microgrids with a high penetration of inverter-coupled energy sources," in *Proc. CIGRE/IEEE PES Joint Symp. Integr. Wide-Scale Renew. Resour. Power Del. Syst.*, Jul. 2009, pp. 1–6.
- [6] E. Casagrande, W. L. Woon, H. H. Zeineldin, and D. Svetinovic, "A differential sequence component protection scheme for microgrids with inverter-based distributed generators," *IEEE Trans. Smart Grid*, vol. 5, no. 1, pp. 29–37, Jan. 2014.
- [7] S. R. Samantaray, G. Joos, and I. Kamwa, "Differential energy based microgrid protection against fault conditions," in *Proc. IEEE PES Innov. Smart Grid Technol. (ISGT)*, Jan. 2012, pp. 1–7.
- [8] E. Sortomme, S. S. Venkata, and J. Mitra, "Microgrid protection using communication-assisted digital relays," *IEEE Trans. Power Del.*, vol. 25, no. 4, pp. 2789–2796, Oct. 2010.
- [9] L. Liu, Z. Liu, M. Popov, P. Palensky, and M. A. M. van der Meijden, "A fast protection of multi-terminal HVDC system based on transient signal detection," *IEEE Trans. Power Del.*, vol. 36, no. 1, pp. 43–51, Feb. 2021.
- [10] M. Pirani, M. Hosseinzadeh, J. A. Taylor, and B. Sinopoli, "Optimal active fault detection in inverter-based grids," *IEEE Trans. Control Syst. Technol.*, vol. 31, no. 3, pp. 1411–1417, May 2023.
- [11] Z. Gao, C. Cecati, and S. X. Ding, "A survey of fault diagnosis and fault-tolerant techniques—Part I: Fault diagnosis with model-based and signal-based approaches," *IEEE Trans. Ind. Electron.*, vol. 62, no. 6, pp. 3757–3767, Jun. 2015.
- [12] W. Gao, X. Liu, and M. Z. Chen, "Unknown input observer-based robust fault estimation for systems corrupted by partially decoupled disturbances," *IEEE Trans. Ind. Electron.*, vol. 63, no. 4, pp. 2537–2547, Apr. 2015.
- [13] M. Nyberg and E. Frisk, "Residual generation for fault diagnosis of systems described by linear differential-algebraic equations," *IEEE Trans. Autom. Control*, vol. 51, no. 12, pp. 1995–2000, Dec. 2006.
- [14] P. Mohajerin Esfahani and J. Lygeros, "A tractable fault detection and isolation approach for nonlinear systems with probabilistic performance," *IEEE Trans. Autom. Control*, vol. 61, no. 3, pp. 633–647, Mar. 2016.
- [15] K. Pan, P. Palensky, and P. M. Esfahani, "Dynamic anomaly detection with high-fidelity simulators: A convex optimization approach," *IEEE Trans. Smart Grid*, vol. 13, no. 2, pp. 1500–1515, Mar. 2022.
- [16] J. Dong, A. S. Kolarjani, and P. M. Esfahani, "Multimode diagnosis for switched affine systems with noisy measurement," *Automatica*, vol. 151, May 2023, Art. no. 110898.
- [17] C. van der Ploeg, M. Alirezaei, N. van de Wouw, and P. M. Esfahani, "Multiple faults estimation in dynamical systems: Tractable design and performance bounds," *IEEE Trans. Autom. Control*, vol. 67, no. 9, pp. 4916–4923, Sep. 2022.
- [18] C. van der Ploeg, E. Silvas, N. van de Wouw, and P. M. Esfahani, "Real-time fault estimation for a class of discrete-time linear parameter-varying systems," *IEEE Control Syst. Lett.*, vol. 6, pp. 1988–1993, 2022.
- [19] R. H. Park, "Two-reaction theory of synchronous machines generalized method of analysis-part I," *Trans. Amer. Inst. Electr. Engineers*, vol. 48, no. 3, pp. 716–727, Jul. 1929.
- [20] A. Kahrobaei and Y. A. I. Mohamed, "Interactive distributed generation interface for flexible micro-grid operation in smart distribution systems," *IEEE Trans. Sustain. Energy*, vol. 3, no. 2, pp. 295–305, Apr. 2012.
- [21] V. P. Singh, N. Kishor, and P. Samuel, "Distributed multi-agent system-based load frequency control for multi-area power system in smart grid," *IEEE Trans. Ind. Electron.*, vol. 64, no. 6, pp. 5151–5160, Jun. 2017.
- [22] Y. Xu, "Robust finite-time control for autonomous operation of an inverter-based microgrid," *IEEE Trans. Ind. Informat.*, vol. 13, no. 5, pp. 2717–2725, Oct. 2017.
- [23] S. X. Ding, *Model-based Fault Diagnosis Techniques: Design Schemes, Algorithms, and Tools*. Cham, Switzerland: Springer, 2008.
- [24] J. Dong, Y. Liao, H. Xie, J. Cremer, and P. M. Esfahani, "Real-time ground fault detection for inverter-based microgrid systems," 2023, *arXiv:2304.12445*.
- [25] R. Podmore and M. R. Robinson, "The role of simulators for smart grid development," *IEEE Trans. Smart Grid*, vol. 1, no. 2, pp. 205–212, Sep. 2010.
- [26] N. Pogaku, M. Prodanovic, and T. C. Green, "Modeling, analysis and testing of autonomous operation of an inverter-based microgrid," *IEEE Trans. Power Electron.*, vol. 22, no. 2, pp. 613–625, Mar. 2007.
- [27] J. Löfberg, "YALMIP: A toolbox for modeling and optimization in MATLAB," in *Proc. CACSD Conf.*, Taipei, Taiwan, 2004, pp. 284–289.